Inversing the natural hydrogen bonding rule to selectively amplify GC-rich ADAR-edited RNAs.

Rodolphe Suspène, Myrtille Renard, Michel Henry, Denise Guétard, David Puyraimond-Zemmour, Agnès Billecocq, Michèle Bouloy, Frederic Tangy, Jean Pierre Vartanian, Simon Wain-Hobson

HAL Id: pasteur-00285811
https://pasteur.hal.science/pasteur-00285811

Submitted on 27 Jun 2008

Nucleic Acids Research

Supplement/Special Issue	This article is part of the following issue: *"Supplementary Data"* **http://nar.oxfordjournals.org/cgi/content/full/gkn295/DC1** The full text of this article, along with updated information and services is available online at http://nar.oxfordjournals.org/cgi/content/full/gkn295v2
References	This article cites 54 references, 22 of which can be accessed free at http://nar.oxfordjournals.org/cgi/content/full/gkn295v2#BIBL
Supplementary material	Data supplements for this article are available at http://nar.oxfordjournals.org/cgi/content/full/gkn295/DC1
Reprints	Reprints of this article can be ordered at http://www.oxfordjournals.org/corporate_services/reprints.html
Email and RSS alerting	Sign up for email alerts, and subscribe to this journal's RSS feeds at http://nar.oxfordjournals.org
PowerPoint® image downloads	Images from this journal can be downloaded with one click as a PowerPoint slide.
Journal information	Additional information about Nucleic Acids Research, including how to subscribe can be found at http://nar.oxfordjournals.org
Published on behalf of	Oxford University Press http://www.oxfordjournals.org

Inversing the natural hydrogen bonding rule to selectively amplify GC-rich ADAR-edited RNAs

Rodolphe Suspène[1,2], Myrtille Renard[1,2], Michel Henry[1,2], Denise Guétard[1,2], David Puyraimond-Zemmour[1,2], Agnès Billecocq[3], Michèle Bouloy[3], Frederic Tangy[2,4], Jean-Pierre Vartanian[1,2] and Simon Wain-Hobson[1,2,*]

[1]Unité de Rétrovirologie Moléculaire, [2]CNRS URA 3015, [3]Unité de Génétique Moléculaire des Bunyaviridés and [4]Laboratoire de Génomique Virale et Vaccination, Institut Pasteur, 28 rue du Dr Roux, 75724 Paris cedex 15

ABSTRACT

DNA complementarity is expressed by way of three hydrogen bonds for a G:C base pair and two for A:T. As a result, careful control of the denaturation temperature of PCR allows selective amplification of AT-rich alleles. Yet for the same reason, the converse is not possible, selective amplification of GC-rich alleles. Inosine (I) hydrogen bonds to cytosine by two hydrogen bonds while diaminopurine (D) forms three hydrogen bonds with thymine. By substituting dATP by dDTP and dGTP by dITP in a PCR reaction, DNA is obtained in which the natural hydrogen bonding rule is inversed. When PCR is performed at limiting denaturation temperatures, it is possible to recover GC-rich viral genomes and inverted Alu elements embedded in cellular mRNAs resulting from editing by dsRNA dependent host cell adenosine deaminases. The editing of Alu elements in cellular mRNAs was strongly enhanced by type I interferon induction indicating a novel link mRNA metabolism and innate immunity.

INTRODUCTION

It is a truism that a GC base pair has three hydrogen bonds while AT has two. In fact, Watson and Crick did not quite see it that way back in 1953 (1,2). It was Pauling and Corey who demonstrated the validity of the third hydrogen bond in the GC pair in 1956 (3). The third hydrogen bond helps understand why GC-rich DNA melts at higher temperatures compared to AT-rich DNA. Indeed, when performing PCR on GC-rich segments the denaturation temperature is sometimes increased to ensure complete melting (4).

Generally speaking, the denaturation temperature has not been considered as a variable in PCR. Recently, lower denaturation temperatures were exploited to selectively amplify so-called G→A hypermutants of the human immunodeficiency virus (HIV) (5). They arise from genetic editing of nascent viral cDNA by two host cell cytidine deaminases of the APOBEC3 family (6–11). Deamination of numerous cytidine (C) residues on the viral minus strand yields multiple uracil (U) residues, which are copied as a thymidine (T). With respect to the viral plus strand as reference, these show up as genomes with numerous G→A transitions giving rise to the term G→A hypermutants (12,13). Temperature differences as small as 1–2°C were enough to allow differential amplification of A rich hypermutants in the presence of as much as 10^4 fold excess of wild type, or reference genomes (14,15). The method was referred to as differential DNA denaturation PCR, or 3D-PCR for short (5). Obviously the converse is not possible, that is selective amplification of GC-rich alleles with respect to a reference clone, because such alleles would melt at even higher temperatures.

This not a moot point in virology for example, where there are examples of A→G hypermutated RNA viral genomes, the paradigm being measles virus (MV). Such genomes have been identified in autopsy samples from cases of MV-associated subacute sclerosing panecephalitis and inclusion body encephalitis (16). They arise from deamination of numerous adenosine residues in the context of double stranded RNA (dsRNA) by host cell adenosine deaminases of the ADAR family [for review see (17)]. Editing of adenosine yields inosine (I). As I hydrogen bonds essentially as guanosine (G), edited RNA sequences are recovered as G-rich alleles. The extent of editing may vary from a few bases to up to 50% of potential target adenosine residues (18,19).

Of the two ADAR1 gene transcripts ADAR-1L and -1S, only the former can be induced by interferon α/β and γ (20). Despite this, the number of examples of ADAR edited RNA viral sequences has remained little more than a handful, being confined mainly to negative stranded viruses such as vesicular stomatitis virus, respiratory syncytial virus and paramyxovirus (19,21,22) the signal

*To whom correspondence should be addressed. Tel: +33 1 45 68 88 21; Fax: +33 1 45 68 88 74; Email: simon@pasteur.fr
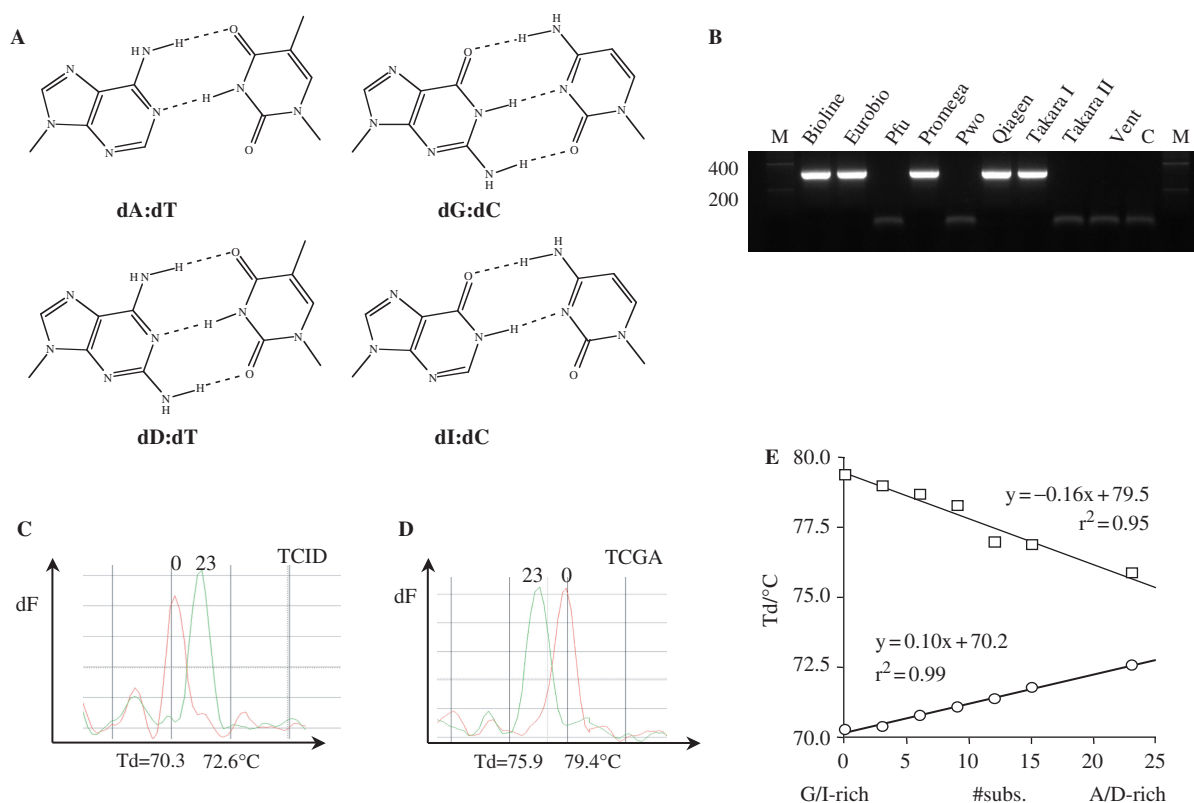
Figure 1. The basis of selective amplification of GC-rich alleles. (**A**) Base pairing of standard and DNA base pairs as well as those involving inosine (I) and diaminopurine (D). (**B**) Five of 8 commercially available thermostable polymerases can efficiently incorporate dITP and dDTP into DNA. dNTP concentrations were 200 µM throughout, $[Mg^{2+}] = 2.5$ mM, Td = 95°C. C = negative buffer control, M = markers in bps. The input material was DNA corresponding to the reference sequence (34% GC) in Supplementary Figure 1. The Bioline, Eurobio, Promega, Qiagen and Takara enzymes are all variants of Taq polymerase. Takara I and II refer to two buffers supplied by the manufacturer. At 20 cycles the Bioline enzyme gave better product yield and was therefore used in all subsequent work. (**C**) SYBR Green melting profiles for TCGA DNA corresponding to the HIV-1 V1V2 region fragments. The reference is marked '0' while '23' denotes the clone differing uniquely by 23 G→A transitions. Midpoint Tds are given below the x-axis. (**D**) SYBR Green melting profiles for TCID DNA corresponding to the HIV-1 V1V2 region fragments. Midpoint Tds are given below the x-axis. (**E**) Linear correlations between midpoint Tds and G/I or A/D composition of 7 HIV-1 clones whose sequences are given in Supplementary Figure 1.

exception being measles virus *in vivo*. The genome of the hepatitis D satellite virus may also be edited by ADAR-1L (23).

With the explosion of information on small cellular RNA molecules, it is recognized that many fold up into tight rod like structures (24,25). Some micro and siRNAs undergo adenosine editing yielding the characteristic A→G transition when recovered as cloned DNA (26–32).

Large numbers of Alu retroelements are found in genes (33,34). When two are inserted in opposite orientations, the inverted Alu RNAs hybridize forming long dsRNA duplexes, which are substrates for ADARs (35–39). While inverted Alus can be found in introns, they are generally embedded in the 3′ non-coding region of the mRNAs. Through massive and labour intensive EST studies and bioinformatics comparisons with the human genome it is known that hundreds of human mRNAs undergo A→I editing (35,38,39).

Given the emerging importance of ADAR editing of a wide variety of RNAs (40–42), it would be useful to have a PCR based method to allow selective amplification of GC-rich alleles. In view of the 3:2 hydrogen bonding rule for GC and AT base pairs, differential denaturation of target DNA would appear to be out of the question. Yet the beginnings to a solution lie in ADAR editing itself. Inosine base pairs with cytidine through two hydrogen bonds rather than the three typical for a GC base pair (Figure 1A).

Modified bases are often encountered in DNA bacteriophage genomes, usually as a means to avoid host restriction enzymes (43). Invariably modifications involve cytidine or thymidine, for example 5-hydroxymethyl cytidine in phage T4 DNA. There is however, just one example of a modified purine, 2,6-diaminopurine (44), or 'D'. It is found in the cyanophage S-2L DNA genome where it totally substitutes for adenosine and has the singular feature of base pairing with thymine (T) via three hydrogen bonds (Figure 1A). As dITP and dDTP are commercially available, the outlines of a PCR based method allowing selective amplification of GC-rich alleles becomes clear—a combination of differential denaturation PCR using the modified bases dITP and dDTP. Does it work?

MATERIALS AND METHODS

Viruses

MRC5 and Vero cells were grown in Dulbecco's modified Eagle's medium containing 5–10% fetal calf serum and antibiotics (5 U/ml penicillin and 5 µg/ml streptomycin) in the presence of 5% CO_2. Cell monolayers in 6-well plates were infected with live attenuated measles virus (Schwarz strain amplified on Vero cells) at a multiplicity of infection of 0.1 for Vero cells and 3 for MRC-5. Two days after infection culture medium was collected and cells were trypsinized. After clarification of cell debris, RNA was extracted. Subconfluent monolayers were infected with RVFV clone 13 at a multiplicity of infection of 0.01 pfu per cell and incubated for 3 days at 37°C.

RNA extraction, oligonucleotides and PCR reagents and cloning

Samples including cell lysates and viral supernatants were digested in SDS/proteinase K buffer (0.1 mg/ml, Eurobio) at 56°C for 2 h. Total nucleic acids were extracted using the MasterPure complete DNA and RNA purification kit (Epicentre) according to the manufacturer's procedure. Total RNA was then reverse transcribed in a final volume of 20 µl of a mixture containing 1 × buffer reaction (Gibco), 300 ng of random hexamers (Pharmacia), 500 µM each standard dNTP, 10 U of MLV reverse transcriptase (Invitrogen) and 10 U RNAsin (Promega). Ten percent of the reaction was used for PCR amplification.

A fragment of the M gene of MV and of the L gene of RVFV clone 13 was amplified by a nested procedure. To increase sensitivity and specificity, a hot-start PCR was performed for both amplifications. First-round primers for MV were 5ROUout and 3ROUout, respectively 5′ GG CAGGCYGGYGCCCCAGGYCAGAG and 5′GGRR CCTCTGCGGGGGTRTCGRGCGG, and maps to 3522-3903 on the Schwarz genome. For the second round, primers were 5ROUin and 3ROUin, respectively 5′AGA YCCYGGYCYAGGCGACAGGAAGG and 5′GCR TTGCRCRCTTGGTTTGCGTTG, where Y = T/C and R = A/G. First-round primer for RVFV amplification were 5RFout and 3RFout, respectively 5′GTCGCCAATGY CGAGGAGGCCCAYGA and 5′CTCCAGATCATCT RTCCTRRTGCTTCC, and map to 5872-6255 on the L fragment of RVFV. For the second round, primers were 5RFin and 3RFin, respectively 5′GATGATAGAAG AYGCCAAGAACAAYGC and 5′TGCTTCCTTCTGG TCTCTGTRGRGTTC.

Standard dNTPs were purchased from Sigma and dDTP, dITP, dUTP, 5Me-dCTP were purchased from TriLink. DAPI was from Fluka while 7-deazadGTP and the Hoechst bisbenzamide dye (H33258) were from Sigma. PCR products were purified from agarose gels and ligated into the TOPO TA cloning vector cloned and sequenced as described (5).

PCR protocol

Hypermutated genomes were identified by a three-step protocol. The first reaction involved a standard amplification of PCR to generate sufficient material. Conditions were: 2.5 mM $MgCl_2$, 50 mM KCl, 10 mM Tris-HCl (pH 8.3), 200 µM of dATP, dTTP, dCTP and dGTP, 100 µM each primer and 5 U of BioTaq DNA polymerase (Bioline) in a final volume of 50 µl. The second reaction converted standard DNA to that containing the modified based D and I, referred to as TCID DNA. This is essential because if input material is TCGA DNA, the Tds of GC-rich alleles are governed by the natural base pairing rule and so cannot be differentially amplified. The conditions were as above except that 200 µM each dTTP, dCTP, dDTP and dITP, 100 µM each primer and 10 U of BioTaq DNA polymerase (Bioline) were used in a final volume of 50 µl. The denaturation temperature was 95°C.

Differential amplification was performed in the third round by using an Eppendorf gradient Mastercycler S programmed to generate 2–10°C gradients in the denaturation temperature. The reaction parameters were performed by using, for example, a 8°C denaturation gradient for 5 min, followed by 35 cycles (a 8°C denaturation gradient for 30 s, annealing 55°C for 30 s and constant polymerization temperature equal to the minimum denaturation gradient temperature for 1 min) and finally 10 min at the minimum denaturation gradient temperature to finish elongation. While the magnitude of the denaturation gradient can be changed, the constant polymerization temperature is always equal to the minimum denaturation gradient temperature. The buffer conditions were 2.5 mM $MgCl_2$, 50 mM KCl, 10 mM Tris-HCl (pH 8.3), 200 µM each dTTP, dCTP, dDTP and dITP, 100 µM each primer and 10 U of BioTaq DNA polymerase (Bioline) in a final volume of 50 µl.

Increasing the concentration of dITP and dDTP to 300 µM did not increase product yield (not shown). Although inosine base pairs essentially as guanosine, it can form base pairs with T and A, hence the use of dITP in PCR is somewhat mutagenic. In an attempt to favorize dC:dITP pairing the concentration of dCTP was increased from 200 to 300 µM while the dTTP was lowered to 100 µM and the fidelity compared to that resulting from amplification using equimolar 200 µM dNTPs. As no change in PCR fidelity was found (4.1×10^{-3} versus 3.9×10^{-3} per base), all subsequent amplifications were performed using equimolar dNTPs.

Amplification by 3DI-PCR of cellular mRNA embedded Alu sequences

Total RNA from infected and uninfected MRC5 cells was extracted (Epicentre). cDNA synthesis was performed by using random priming as described above. 1/10 of the cDNA reaction was used for PCR amplification with primers Alu1 (5′ CACGCCTGTAATCCCAGCACTTT GGG) and Alu2 (5′ TGTCGCCCAGGCTGGAGTGC AGTGG). PCR conditions were 95°C for 5 min followed by 35 cycles with 95°C for 30 s, 60°C for 30 s and 72°C for 1 min and a final elongation step of 72°C for 10 min. First PCR was performed with standard dNTPs (TCGA). 1/50 of the first PCR reaction was used for 3DI-PCR with modified dNTPs (TCID) using a Td gradient from 84 to 60°C for 5 min then 45 cycles with 60–84°C for 45 s,

60°C for 45 s and 60–72°C for 1 min. PCR products were purified and cloned as described above.

Amplification of Ig Vk1 sequences from patients 2 and 3

CD14+ B-lymphocytes were purified from two splenectomized patients using a B-cell isolation Kit (Miltenyi Biotec) and DNA extracted (Epicentre). DNA was amplified using primers Ig1 (5′GCGGACATCCAGATGACCCAGTCT) and Ig2 (5′ GCGCTGTTGACAGTARTAAGTTGCA). Amplification conditions were: 95°C for 5 min, then 35 cycles with 95°C for 30 s, 60°C for 30 s and 72°C for 1 min 1/50 of the PCR product was used for respectively 3D-PCR and 3DI-PCR. For 3D-PCR conditions were, 74–94°C for 5 min then 74–94°C for 1 min 55°C for 30 s and 72°C for 1 min for 35 cycles, and for 3DI-PCR conditions were, 60–75°C for 5 min followed by 60–75°C for 30 s, 55°C for 30 s and 60–75°C for 1 min with 35 cycles and a final elongation step of 60–75°C for 10 min 3D- and 3DI-PCR products were purified and cloned as described above.

RESULTS

A wide variety of thermostable DNA polymerases were first screened for their ability to amplify DNA using dTTP, dCTP, dITP and dDTP. Using a standard buffer and a 95°C denaturation temperature, five of eight thermostable polymerases resulted in reasonable product recovery after 30 cycles using an extended elongation time of 1 min (Figure 1B). All five were commercial variants of Taq polymerase. However, product recovery was ∼3-fold compared to amplification using dGTP and dATP.

The denaturation properties of PCR DNA containing the two modified bases (TCID DNA) were established for a series of seven 262 bp DNA fragments that differed only by up to 23 G→A transitions distributed across the locus (Supplementary Figure 1). As can be seen from SYBR Green melting profiles, midpoint denaturation temperatures (Td) of 70.3 and 72.6°C were obtained for TCID DNA corresponding to the reference (0) and 23 base variant respectively, as anticipated from the change in hydrogen bonding patterns (Figure 1C). As expected for standard PCR products (i.e. TCGA DNA), the converse prevailed, i.e. the A-rich allele was denatured at a lower temperature, Td = 75.9°C, than the G-rich allele (79.4°C, Figure 1D). The midpoint Tds of the seven

molecular clones varied linearly with G/I or A/D content (Figure 1E). The temperature sensitivity of TCID DNA as a function of G/I content was only ∼60% that of TCGA DNA.
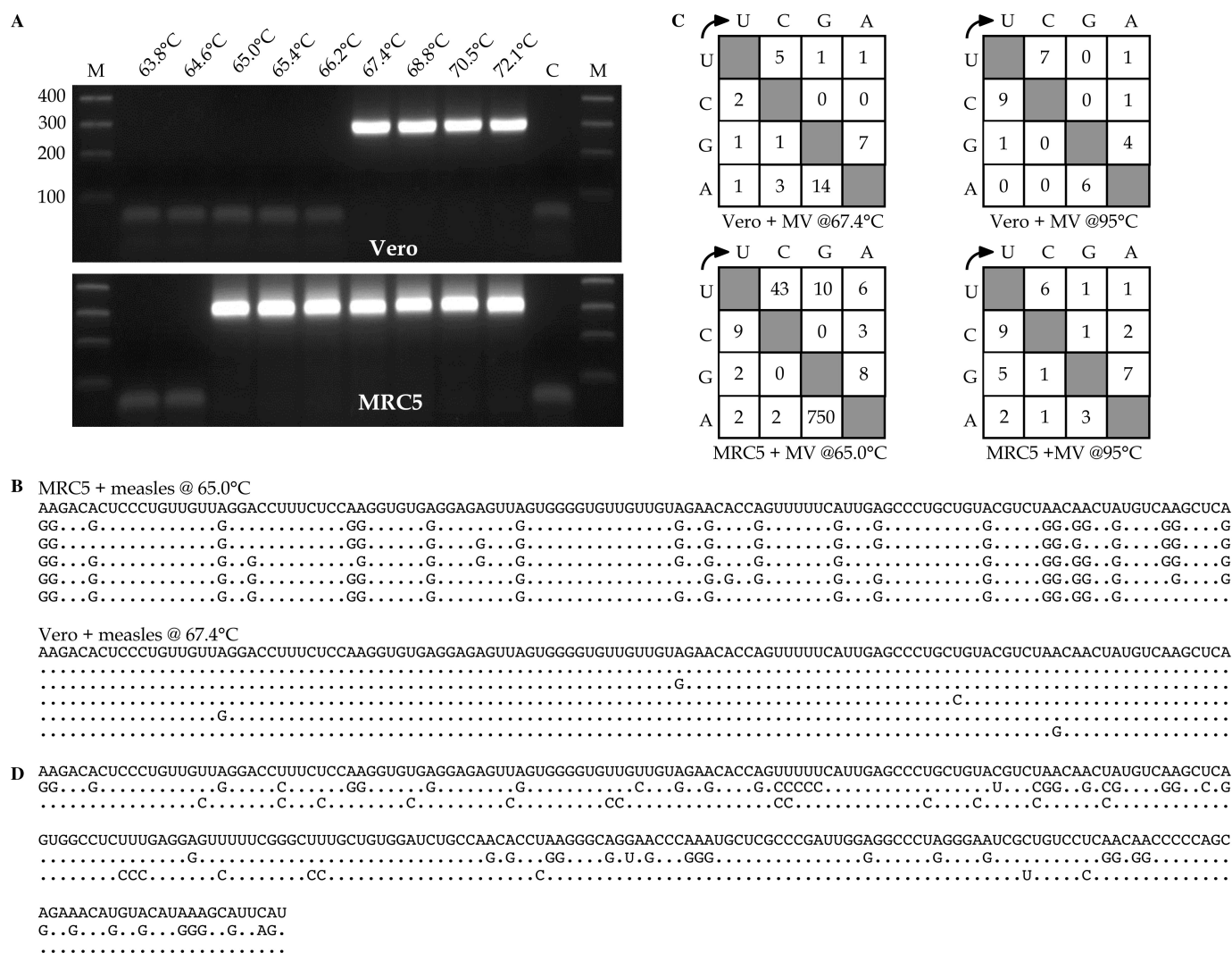
We explored a variety of PCR conditions to try and manipulate the denaturation sensitivity of TCID DNA. Despite trying a range of small organic molecules that bind to AT motifs via the minor groove, i.e. Hoechst bisbenzmide dye H33258, modified bases such as dUTP, 5-MedCTP and 7-deazadGTP, monovalent (K^+) and divalent cations (Mn^{2+}), none had any significant impact on the minimal denaturation temperature/base composition relationship of the seven standards (Figure 2 and not shown). In short, while the overall Td can indeed be manipulated, the denaturation temperature/base composition relationship of TCID DNA is relatively refractory to manipulation.

Recovery of *in vitro* hyperedited measles virus sequences

We sought to validate the method using measles virus (MV) samples grown in the interferon sensitive cell line MRC-5. As a control Vero cells were used which are defective for interferon-a and b production (45). The attenuated MV Schwarz strain was used because it is a good inducer of interferon (46). Two days post-infection supernatant and cell pellets were collected and total RNA extracted. Complementary DNA was converted into PCR products, a fraction of which was converted into TCID PCR products using a 95°C denaturation temperature. Selective amplification was then applied to the TCID DNA using a denaturation gradient of 63–72°C. As can be seen from Figure 3A the minimum temperature at which MV genomes were amplified from Vero cells was 67.4°C. By contrast MV specific products were amplified from the MRC-5 cells down to 65°C. TCID products amplified at the lowest Td were used for molecular cloning into TOPO plasmids. Probably in view of the unusual bases, transformation of standard bacteria with cloned TCID products not only gave very low efficiencies (<500-fold lower than TCGA DNA) but also was invariably accompanied by large deletions within the MV sequences. To overcome this, a fraction of TCID PCR products was converted into standard DNA by 10 cycles of PCR using normal dNTPs and then cloned. As controls, DNA
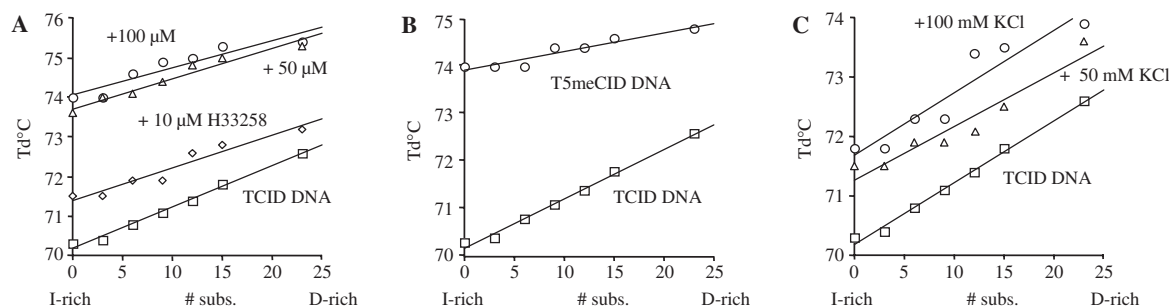
Figure 2. The temperature differential of TCID DNA is relatively refractory to manipulation. (**A**) Hoechst bisbenzmide dye H33258 that binds to AT-rich DNA via the minor groove increases the Td but not the temperature differential. (**B**) Substituting modified bases such as 5-MedCTP for dCTP, dUTP for dTTP and 7-deazadGTP for dGTP (not shown) also failed to increase the temperature differential of TCID DNA. (**C**) Increasing the ionic strength by the addition of monovalent (K^+) and divalent cations (Mn^{2+}, not shown) failed to increase the temperature differential.

A

C

↱	U	C	G	A
U		5	1	1
C	2		0	0
G	1	1		7
A	1	3	14	

Vero + MV @67.4°C

↱	U	C	G	A
U		7	0	1
C	9		0	1
G	1	0		4
A	0	0	6	

Vero + MV @95°C

↱	U	C	G	A
U		43	10	6
C	9		0	3
G	2	0		8
A	2	2	750	

MRC5 + MV @65.0°C

↱	U	C	G	A
U		6	1	1
C	9		1	2
G	5	1		7
A	2	1	3	

MRC5 +MV @95°C

B MRC5 + measles @ 65.0°C
```
AAGACACUCCCUGUUGUUAGGACCUUUCUCCAAGGUGUGAGGAGAGUUAGUGGGGUGUUGUUGUAGAACACCAGUUUUUCAUUGAGCCCUGCUGUACGUCUAACAACUAUGUCAAGCUCA
GG...G............G..............GG......G........G.........G..G....G.......G...G............G.....GG.GG..G....GG....G
GG...G.............G..........GG.....G....G...G..........G..G....G.......G...G............G.....GG.G...G....GG....G
GG...G............G..G.........G.....G...G...G..........G..G....G.......G...G............G.....GG.GG..G...G.......G
GG...G............G..G.........GG.....G....G.........G...G.G..G............G...G............G.....GG.GG..G...G....G
GG...G............G...G.........GG......G....G.........G...G............G...G............G.....GG.GG..G.........
```

Vero + measles @ 67.4°C
```
AAGACACUCCCUGUUGUUAGGACCUUUCUCCAAGGUGUGAGGAGAGUUAGUGGGGUGUUGUUGUAGAACACCAGUUUUUCAUUGAGCCCUGCUGUACGUCUAACAACUAUGUCAAGCUCA
......................................................................................................................
...............................................................................G......................................
...................................................................................................C..................
..............G.......................................................................................................
...........................................................................................................G..........
```

D
```
AAGACACUCCCUGUUGUUAGGACCUUUCUCCAAGGUGUGAGGAGAGUUAGUGGGGUGUUGUUGUAGAACACCAGUUUUUCAUUGAGCCCUGCUGUACGUCUAACAACUAUGUCAAGCUCA
GG...G...........G.....C......GG.....G........G..........C...G..G....G.CCCCC...............U...CGG..G.CG....GG..C.G
...............C.......C...C........C.........C.........CC...............CC...........C....C.....C......C...........
```
```
GUGGCCUCUUUGAGGAGUUUUUCGGGCUUUGCUGUGGAUCUGCCAACACCUAAGGGCAGGAACCCAAAUGCUCGCCCGAUUGGAGGCCCUAGGGAAUCGCUGUCCUCAACAACCCCCAGC
.................G......................................G.G...GG....G.U.G...GGG...............G......G...G.........GG.GG...
.......CCC.......C........CC.....................C..........................................U.....C..............
```
```
AGAAACAUGUACAUAAAGCAUUCAU
G..G...G..G...GGG..G..AG.
.........................
```

Figure 3. 3DI-PCR amplification of ADAR edited measles virus genomes. (**A**) Agarose gel of TCID DNA amplified from measles infected Vero and MRC-5 cells. The PCR products amplified from the latter between 65 and 66.2°C are indicative of genomes enriched in GC. C, negative buffer control; M molecular weight markers. (**B**) MV sequences derived from amplification at the lowest denaturation temperature (65°C). Sequences are aligned to the reference MV sequence, only differences being shown. The monotonous A→G transitions are typical of ADAR editing. Complete sequence sets are given in Supplemental Figure 2. (**C**) Mutation matrices for the sequence sets. The number of sequences per matrix is, starting top left and going clockwise $n = 15$, 13, 21 and 19. The symmetry of the matrices 95°C amplification controls is typical of a viral quasispecies. A slight skew in the Vero/MV 67.4°C matrix from AU→GC is understandable given that 3DI-PCR amplifies GC-rich sequences, and represents the GC-rich end of the mutant spectrum. (**D**) Sequences of two C-rich MV sequences compared to the reference genome. The first encodes A→G and U→C transitions and arises from editing of the viral genome and anti-genome, while the latter U→C transitions indicating editing only of the anti-genome.

amplified from reactions using a Td = 95°C was also cloned and sequenced.

As can be seen from Figures 3B and Supplementary Figure 2, the MV genomes selectively amplified from MRC-5 cells (Td = 65°C) were littered with A→G transitions. Indeed, up to 83% of A residues could be edited (mean = 70%, range 3–83%). By contrast, those amplified from MV-infected Vero cells at the lowest possible temperature (Td = 67.4°C) were typical of quasispecies variation of an RNA virus. MV sequences amplified under standard PCR conditions (Td = 95°C, normal dNTPs) showed balanced mutation matrices (Figure 3C). This indicates that the highly edited sequences from the MRC-5 cell line must represent a subset, and that the selective PCR

protocol was indeed capable of recovering GC-rich alleles. Two cytidine-rich MV sequences compared to the reference genome were identified (Figure 3D). The first encoded A→G and U→C transitions and probably arose from editing of the viral genome and anti-genome, while the latter sequence encoding only U→C transitions was presumably derived from editing of mRNA or the anti-genome.

To ascertain their frequency, the initial TCID products were serially diluted and standard and selective PCR performed. The signal from standard PCR titrated out 100-fold further than selective PCR indicating that the highly edited genomes were present in the sample at ∼1% (data not shown). A→G hypermutants were also found in

viral supernatants from MV-infected MRC-5 cells indicating that hyperedited genomes can be packaged and raises the possibility that editing might continue within the virion (Supplementary Figure 3).

We refer to this novel method as inverse differential DNA denaturation PCR, or 3DI-PCR, to distinguish it from 3D-PCR that allows amplification of AT-rich DNA (5).

### Genetic editing of a segmented RNA virus

In order to see if 3DI-PCR could be applied to another viral system and hence generate novel findings, we analysed Rift Valley fever virus (RVFV), a segmented negative stranded RNA virus. Currently, there are no reports of ADAR edited RVFV genomes. RVFV clone 13 is a highly immunogenic, yet attenuated strain that encodes a 549 bp in frame deletion within the NSs gene. As the vestigial NSs protein has lost its ability to antagonize interferon production, clone 13 is a good inducer of interferon, unlike virulent strains (47). While clone 13 grew well on Vero cells, viral titers were ~100-fold lower on MRC-5 cells.

Clone 13 was cultured on both cell lines for 3 days and total cellular RNA recovered. Using primers specific for a 257 bp fragment from the L gene, 3DI-PCR could recover RVFV genomes at a lower temperature from the restrictive MRC-5 culture compared to the permissive Vero cell culture, 66.3°C compared to 67.2°C (Figure 4A). Cloning and sequencing of the PCR products revealed extensive A→G editing of viral RNA from the MRC-5 culture and nothing more than a quasispecies variation from the Vero cells (Figure 4B and C). Although a handful of hyperedited sequences are shown, all 26 clones derived from the MRC-5 infection were distinct and harbored between 63 and 77% of edited adenosine targets. Thus hyperediting of RVFV RNA in MRC-5 can be just as extensive as for MV in the same cell line. When analysed by standard PCR (Td = 95°C, normal dNTPs) the mutation matrices were balanced, indicating that the highly edited RVFV genomes identified represent a minority (Figure 4C). Complete RVFV sequence sets can be found in Supplemental Figure 4.
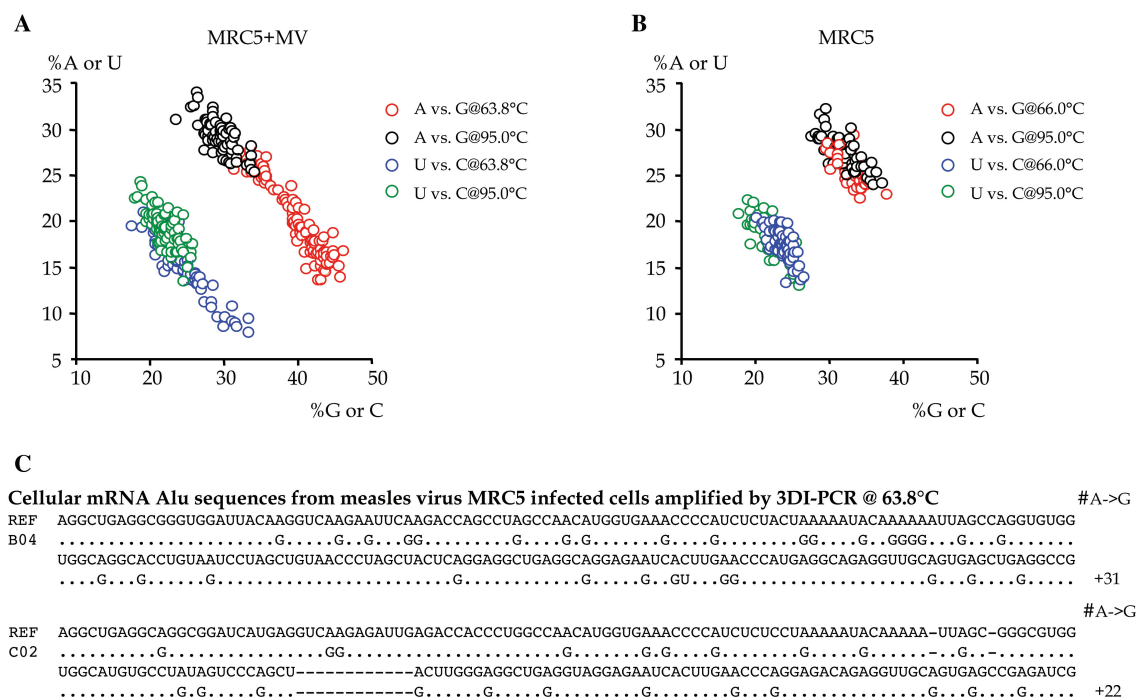
Selective amplification of edited Alu elements in mRNA

By comparison of EST sequence libraries and genome sequences several reports have shown that inverted Alu elements embedded in cellular mRNAs can undergo ADAR editing (26,35,37,38,48). We decided to see if 3DI-PCR could supplant such powerful, yet brut force approaches. Randomly primed cDNA from MV infected MRC-5 cells was used, as there was *prima face* evidence
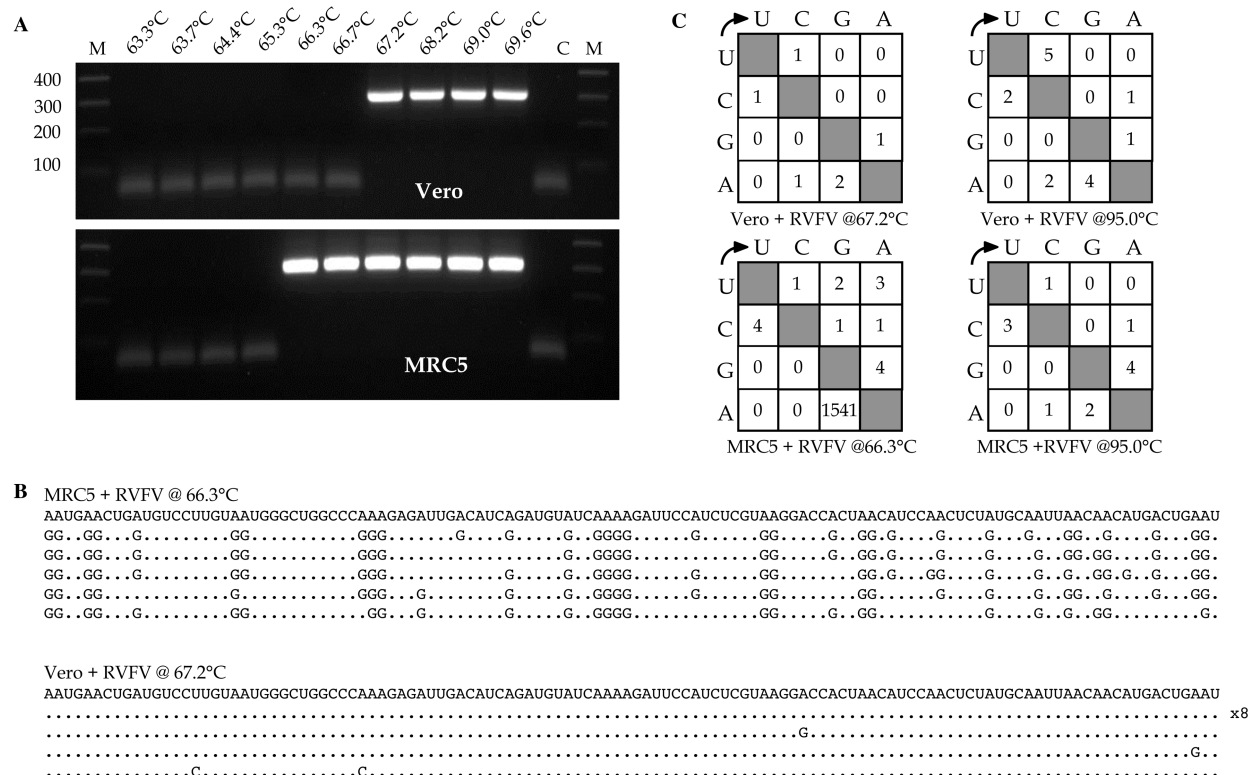
Figure 4. Massive adenosine deamination of Rift valley fever virus genomes. RVFV clone 13 is a highly immunogenic yet attenuated strain that encodes a 549 bp in frame deletion within the NSs gene. As the vestigial NSs protein has lost its ability to antagonize interferon production, clone 13 is a good inducer of interferon, unlike virulent strains (47). While clone 13 grows well on Vero cells, viral titres were 100-fold lower on MRC-5 cells. (**A**) Agarose gel of TCID DNA amplified from RVFV infected Vero and MRC-5 cells. The PCR products amplified from the latter between 66.3 and 66.7°C are indicative of genomes enriched in GC. C, negative buffer control; M molecular weight markers. (**B**) RVFV sequences derived from amplification at the lowest denaturation temperature (66.3°C). Sequences are aligned to the reference MV sequence, only differences being shown. The monotonous A→G transitions are typical of ADAR editing. Complete sequence sets are given in Supplementary Figure 4. (**C**) Mutation matrices for the sequence sets. The number of sequences per matrix is, starting top left and going clockwise n = 6, 10, 11 and 26. The symmetry of the matrices 95°C amplification controls is typical of a viral quasispecies.

Figure 5. Selective amplification of ADAR-edited Alu elements nested in cellular mRNAs. (**A**) A versus G base composition (red and black) and U versus C (blue and green) of individual Alu sequences from cellular mRNAs from measles virus (MV) infected MRC-5 cells. Sequences were derived at standard (95°C, $n = 77$ sequences) and restrictive temperatures (63.8°C, $n = 108$ sequences). A versus G correlations pertain to plus sense Alu sequences (%A = −0.996%G + 59.8; $r = 0.915$, $n = 108$, $P = <10^{-3}$) and U versus C (%U = −0.922%C + 38.1; $r = 0.914$, $n = 108$, $P < 10^{-3}$), the anti-sense. The two gradients indicate a strict interconversion of A to G and U to C. (**B**) A versus G and U versus C correlations for Alu sequences derived from cellular mRNA from uninfected MRC5 cells under normal ($n = 58$ sequences) and 3DI-PCR ($n = 67$ sequences). (**C**) Two examples of highly edited Alu elements (B04 and C02) nested within cellular mRNAs. The alignments were those of the best hits derived from blasting the human genome. Only differences are shown to emphasize the effects of ADAR editing. Gaps were introduced into the C02 sequence to allow comparison with the B04 alignment. The number of A→G transitions are shown to the right.
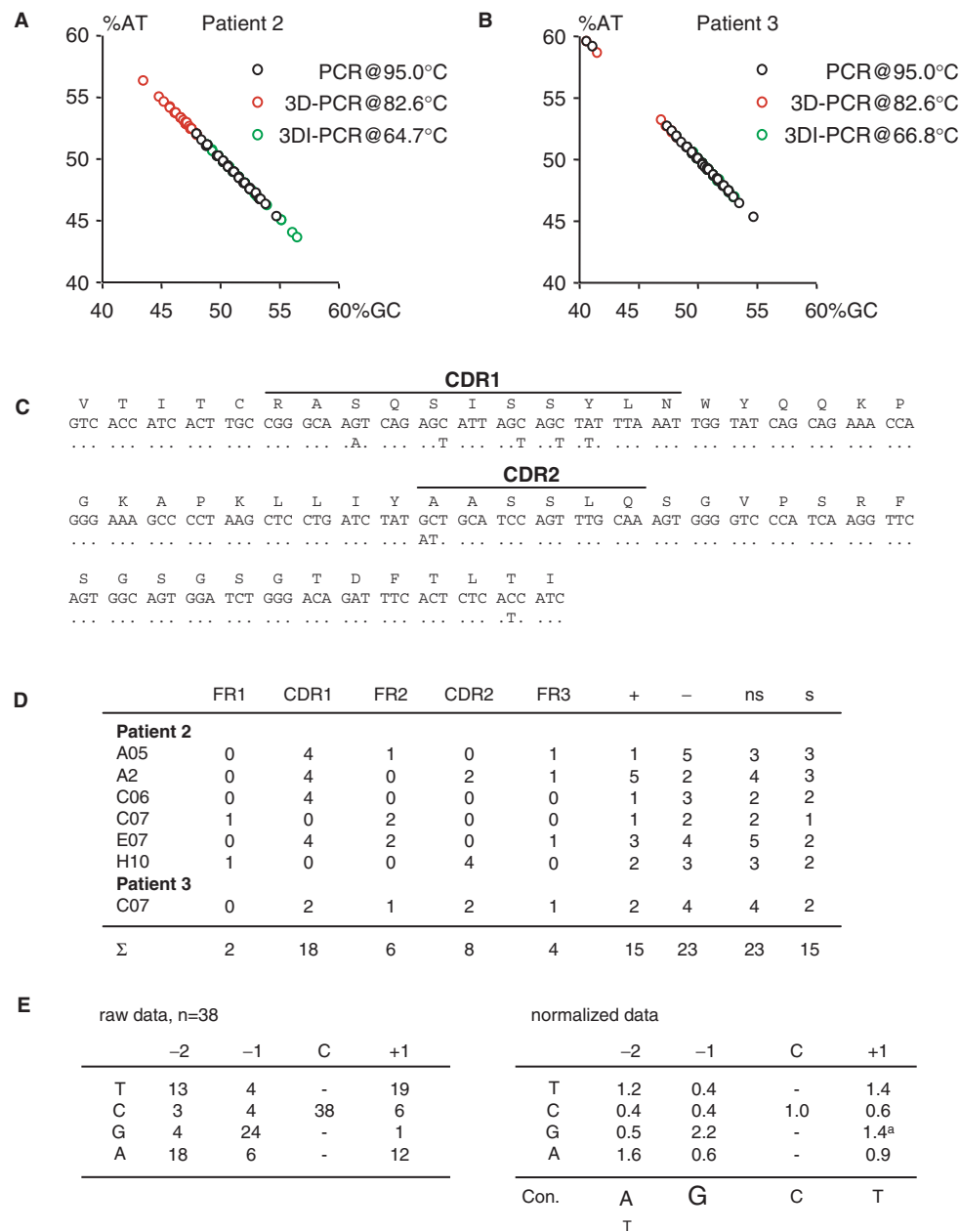
of ADAR activity (Figure 3). Alu-specific primers were chosen corresponding to a region that apparently underwent little ADAR-editing (35,39,49). PCR products were amplified at a temperature as low as 63.8°C. As reflected by their A versus G (+ strand) and U versus C (−strand) base compositions (Figure 5A), there was considerable evidence of G and C enrichment compared to Alu sequences derived from amplification using a 95°C denaturation temperature. Indeed the majority of Alu sequences were enriched in either G or C (Figure 5A). Blast analyses showed that the majority of selectively amplified Alu elements had undergone ADAR-editing (Supplementary Table 1A and B), two of which are shown in Figure 4C. In fact ADAR-1L is induced by type I interferons and was detectable by RT-PCR among MV-infected MRC-5 mRNAs and not from uninfected cells (not shown). Hence, the majority of edited Alu sequences can be ascribed to ADAR-1L. When the same 3DI-PCR protocol was applied to Alu-containing mRNAs from uninfected MRC-5 cells, there were no comet tails out to >40%G or >27%C as noted for MV-infected MRC-5 cells (Figure 5B, Supplementary Table 1A and B).

GC and AT-rich rearranged immunoglobulin V regions

Clearly 3DI-PCR is a robust method and complementary to its sister, 3D-PCR capable of amplifying up AT-rich alleles. To see if a combination of the two techniques could be useful when applied to a complex problem, we took the example of somatic hypermutation of rearranged immunoglobulin variable (V) genes. These loci are subject to somatic hypermutation, initiated by genetic editing of ssDNA in transcription bubbles by activation induced deaminase, AID (50). The process features an initial phase targeting GC base pairs followed by a second targeting AT pairs. Primers were designed to amplify the Vk1 light chain DNA from CD14 positive splenic B cells isolated from two patients with follicular hyperplasia who had undergone splenectomy due to untreatable thrombocytopenia (51). As can be seen from Figure 6A and B, 3DI-PCR failed to amplify highly GC-rich alleles over and above that found by PCR using a denaturation temperature of 95°C (Supplementary Tables 3A and C, 4A and C). By contrast its counterpart, 3D-PCR, recovered a series of AT-rich variants (Figure 6A, Supplementary Tables 3B and 4B).

When blasted against the human genome, seven sequences, one of which is shown in Figure 6C, showed an excess of GC→AT transitions in both strands, most of which were concentrated in the two complementary determining regions, CDR1 and CDR2 (Figure 6D, Supplementary Figure 5). As the nucleotide context surrounding the GC→AT transitions is AGCT (Figure 6E), highly analogous to WRC motif (W = A,T; R = A,G where C is the edited nucleotide) observed for AID on single stranded DNA *in vitro* (52), and identical to that for AID

A %AT Patient 2

○ PCR@95.0°C
○ 3D-PCR@82.6°C
○ 3DI-PCR@64.7°C

B %AT Patient 3

○ PCR@95.0°C
○ 3D-PCR@82.6°C
○ 3DI-PCR@66.8°C

C

CDR1

```
      V   T   I   T   C   R   A   S   Q   S   I   S   S   Y   L   N   W   Y   Q   Q   K   P
     GTC ACC ATC ACT TGC CGG GCA AGT CAG AGC ATT AGC AGC TAT TTA AAT TGG TAT CAG CAG AAA CCA
     ... ... ... ... ... ... ... .A. ... ..T ... ..T ..T .T. ... ... ... ... ... ... ... ...
```

CDR2

```
      G   K   A   P   K   L   L   I   Y   A   A   S   S   L   Q   S   G   V   P   S   R   F
     GGG AAA GCC CCT AAG CTC CTG ATC TAT GCT GCA TCC AGT TTG CAA AGT GGG GTC CCA TCA AGG TTC
     ... ... ... ... ... ... ... ... ... AT. ... ... ... ... ... ... ... ... ... ... ... ...
```

```
      S   G   S   G   S   G   T   D   F   T   L   T   I
     AGT GGC AGT GGA TCT GGG ACA GAT TTC ACT CTC ACC ATC
     ... ... ... ... ... ... ... ... ... ... .T. ... ...
```

D

	FR1	CDR1	FR2	CDR2	FR3	+	−	ns	s
Patient 2									
A05	0	4	1	0	1	1	5	3	3
A2	0	4	0	2	1	5	2	4	3
C06	0	4	0	0	0	1	3	2	2
C07	1	0	2	0	0	1	2	2	1
E07	0	4	2	0	1	3	4	5	2
H10	1	0	0	4	0	2	3	3	2
Patient 3									
C07	0	2	1	2	1	2	4	4	2
Σ	2	18	6	8	4	15	23	23	15

E

raw data, n=38

	−2	−1	C	+1
T	13	4	-	19
C	3	4	38	6
G	4	24	-	1
A	18	6	-	12

normalized data

	−2	−1	C	+1
T	1.2	0.4	-	1.4
C	0.4	0.4	1.0	0.6
G	0.5	2.2	-	1.4[a]
A	1.6	0.6	-	0.9
Con.	A T	G	C	T

Figure 6. Identification of GC and AT-rich rearranged immunoglobulin V region sequences from CD14-purified human B cells. (**A** and **B**) A+T versus G+C correlations of individual V region sequences derived by PCR (black), 3D-PCR (green) and 3DI-PCR (red) from patients 2 and 3. (**C**) Alignment of best Blast match to the human genome for the A2 sequence from patient 2. See Supplemental Tables 3 and 4 for complete analyses. (**D**) The majority of C→T transitions (68%) map to the CDR2 and CDR3 regions even though they comprise only 22.5% of the sequence. ± refers to C→T transitions on the sense and antisense strands. Ns/s refer to non-synonymous and synonymous transitions respectively. (**E**) Sequence context of C→T transitions. The raw data is given for the 38 C→T transitions and normalized to that for the target sequences. For example, the normalized frequency of T at position –2 is the quotient of (12/38)/(32/110), the latter fraction comprises the sense and anti-sense sequences weighted by the fraction of mutations in the sense (+) and anti-sense strands (−) (Figure 6D). [a]The frequency of G at position +1 is very low due to the low CpG content of the human genome. The quotient of 1.4 for G at position +1 is not robust as it reflects the quotient of two small fractions, notably (1/38)/(2/110).

mutational hotspots (50), it is plausible that these sequences represent examples of the initial step in the complex process of somatic hypermutation.

DISCUSSION

Differential DNA denaturation PCR exploits the intrinsic stability of GC base pairs arising from a third hydrogen bond, and allows selective amplification of AT-rich DNA (5). By using modified bases the 3:2 rule can be inversed, allowing selective amplification of GC-rich alleles (Figure 1A, C and D). A range of commercially available Taq polymerases was able to undertake incorporation of the two modified bases, although product yields are somewhat less than when standard dNTPs are used. The magnitude of the temperature/GC content coefficients

for 3D- and 3DI-PCR were not equivalent, the latter being ~60% less than the former (Figure 1D).

When applied to measles virus, the prototype for ADAR edited viral genomes, there was no difficulty in recovering highly edited genomes from the MRC-5 culture (Figure 3). Not only are the MV genomes more extensively edited from cultured virus than *in vivo*, they are more heterogeneous (19). The degree of editing observed here is unprecedented; typically ADAR-edited genomes rarely contained more than 50% of edited adenosines (53). Among the present sequences sets the upper limits were ~77 and 83% for RVFV and MV respectively. Although these RNA sequences can form secondary structures as shown by computer programs such as M-fold, never were ~80% of adenosine residues sequestered in dsRNA.

That such genomes were present at frequencies of ~1% in the MRC-5 culture may help explain why MV A→G hypermutants have not been described before in culture. The finding of numerous A→G hypermutants in culture of RVFV clone 13 is also novel and suggests that similar findings could be obtained with most RNA viruses if grown on interferon sensitive cells.

Why would interferon-induced ADAR-1L target 'only' 1% of genomes? The MV sequence sets shown in Figure 3B were obtained at the lowest positive Td, i.e. 65°C. While not shown here, we know that MV sequences taken from the Td = 66.2°C sample were less extensively substituted suggesting that there is a large range in the degree of editing, probably reflecting varying levels of ADAR-1L expression in individual cells. If larger segments were analysed the proportion of lightly edited sequences would increase. Hence the true number of edited MV genomes is probably >1%. As the genomic mutation rate for MV [~1.4 substitutions per cycle (54)] is close to the error threshold for RNA viruses, a little adenosine deamination should be sufficient to kill the virus (55).

While the fate of ADAR-edited mRNAs is debated, it does appear that it is linked to mRNA turnover (53). The finding that ADAR-editing of cellular mRNAs encoding inverted Alu elements is increased upon interferon induction shows that these dsRNA structures are relatively unprotected by protein (Figure 5). If interferon can impinge on the metabolism of several hundreds of mRNAs, then perhaps it might contribute to IFN-induced cell death.

A combination of both PCR methods can be applied to complex sets of sequences as highlighted by the edited human immunoglobulin genes (Figure 6). They could improve the resolution of metagenomic analyses of bacterial genomes that vary greatly in GC content. As they are PCR based they can identify low frequency components that might otherwise escaped identification.

3DI-PCR is robust and simple to perform, dDTP and dITP being commercially available reagents. It is a trifle longer in that extra PCR steps are necessary to perform the selective amplification as well as to obtain reasonable cloning efficiencies. The PCR denaturation temperature has hitherto remained a constant, understandably so as the aim was to denature all DNA. With the use of modified nucleotides, PCR can now be extended to allow selective amplification of GC-rich DNA.

SUPPLEMENTARY DATA

Supplementary Data are available at NAR Online.

ACKNOWLEDGEMENTS

REFERENCES

1. Watson,J.D. and Crick,F.H. (1953) Genetical implications of the structure of deoxyribonucleic acid. *Nature*, **171**, 964–967.
2. Wain-Hobson,S. (2006) The third Bond. *Nature*, **439**, 539.
3. Corey,R.B. and Pauling,L. (1956) Specific hydrogen-bond formation between pyramidines and purines in deoxyribonucleic acids. *Arch. Biochem. Biophys.*, **65**, 164–181.
4. Smith,S.M., Markham,R.B. and Jeang,K.T. (1996) Conditional reduction of human immunodeficiency virus type 1 replication by a gain-of-herpes simplex virus 1 thymidine kinase function. *Proc. Natl Acad. Sci. USA*, **93**, 7955–7960.
5. Suspene,R., Henry,M., Guillot,S., Wain-Hobson,S. and Vartanian,J.P. (2005) Recovery of APOBEC3-edited human immunodeficiency virus G→A hypermutants by differential DNA denaturation PCR. *J. Gen. Virol.*, **86**, 125–129.
6. Harris,R.S., Bishop,K.N., Sheehy,A.M., Craig,H.M., Petersen-Mahrt,S.K., Watt,I.N., Neuberger,M.S. and Malim,M.H. (2003) DNA deamination mediates innate immunity to retroviral infection. *Cell*, **113**, 803–809.
7. Lecossier,D., Bouchonnet,F., Clavel,F. and Hance,A.J. (2003) Hypermutation of HIV-1 DNA in the absence of the Vif protein. *Science*, **300**, 1112.
8. Mangeat,B., Turelli,P., Caron,G., Friedli,M., Perrin,L. and Trono,D. (2003) Broad antiretroviral defence by human APOBEC3G through lethal editing of nascent reverse transcripts. *Nature*, **424**, 99–103.
9. Mariani,R., Chen,D., Schrofelbauer,B., Navarro,F., Konig,R., Bollman,B., Munk,C., Nymark-McMahon,H. and Landau,N.R. (2003) Species-specific exclusion of APOBEC3G from HIV-1 virions by Vif. *Cell*, **114**, 21–31.
10. Suspène,R., Sommer,P., Henry,M., Ferris,S., Guetard,D., Pochet,S., Chester,A., Navaratnam,N., Wain-Hobson,S. and Vartanian,J.P. (2004) APOBEC3G is a single-stranded DNA cytidine deaminase and functions independently of HIV reverse transcriptase. *Nucleic Acids Res.*, **32**, 2421–2429.
11. Wiegand,H.L., Doehle,B.P., Bogerd,H.P. and Cullen,B.R. (2004) A second human antiretroviral factor, APOBEC3F, is suppressed by the HIV-1 and HIV-2 Vif proteins. *EMBO J.*, **23**, 2451–2458.
12. Pathak,V.K. and Temin,H.M. (1990) Broad spectrum of in vivo forward mutations, hypermutations, and mutational hotspots in a retroviral shuttle vector after a single replication cycle: substitutions, frameshifts, and hypermutations. *Proc. Natl Acad. Sci. USA*, **87**, 6019–6023.
13. Vartanian,J.P., Meyerhans,A., Asjo,B. and Wain-Hobson,S. (1991) Selection, recombination, and G→A hypermutation of human immunodeficiency virus type 1 genomes. *J. Virol.*, **65**, 1779–1788.
14. Suspène,R., Guétard,D., Henry,M., Sommer,P., Wain-Hobson,S. and Vartanian,J.P. (2005) Extensive editing of both hepatitis B virus DNA strands by APOBEC3 cytidine deaminases in vitro and in vivo. *Proc. Natl Acad. Sci. USA*, **102**, 8321–8326.

15. Mahieux,R., Suspène,R., Delebecque,F., Henry,M., Schwartz,O., Wain-Hobson,S. and Vartanian,J.P. (2005) Extensive editing of a small fraction of human T-cell leukemia virus type 1 genomes by four APOBEC3 cytidine deaminases. *J. Gen. Virol.*, **86**, 2489–2494.

16. Schmid,A., Spielhofer,P., Cattaneo,R., Baczko,K., ter Meulen,V. and Billeter,M.A. (1992) Subacute sclerosing panencephalitis is typically characterized by alterations in the fusion protein cytoplasmic domain of the persisting measles virus. *Virology*, **188**, 910–915.

17. Valente,L. and Nishikura,K. (2005) ADAR gene family and A-to-I RNA editing: diverse roles in posttranscriptional gene regulation. *Prog. Nucleic Acid Res. Mol. Biol.*, **79**, 299–338.

18. Cattaneo,R., Schmid,A., Eschle,D., Baczko,K., ter Meulen,V. and Billeter,M.A. (1988) Biased hypermutation and other genetic changes in defective measles viruses in human brain infections. *Cell*, **55**, 255–265.

19. Bass,B.L., Weintraub,H., Cattaneo,R. and Billeter,M.A. (1989) Biased hypermutation of viral RNA genomes could be due to unwinding/modification of double-stranded RNA. *Cell*, **56**, 331.

20. Samuel,C.E. (2001) Antiviral actions of interferons. *Clin. Microbiol. Rev.*, **14**, 778–809.

21. O'Hara,P.J., Nichol,S.T., Horodyski,F.M. and Holland,J.J. (1984) Vesicular stomatitis virus defective interfering particles can contain extensive genomic sequence rearrangements and base substitutions. *Cell*, **36**, 915–924.

22. Rueda,P., Garcia-Barreno,B. and Melero,J.A. (1994) Loss of conserved cysteine residues in the attachment (G) glycoprotein of two human respiratory syncytial virus escape mutants that contain multiple A-G substitutions (hypermutations). *Virology*, **198**, 653–662.

23. Chang,J., Gudima,S.O. and Taylor,J.M. (2005) Evolution of hepatitis delta virus RNA genome following long-term replication in cell culture. *J. Virol.*, **79**, 13310–13316.

24. Birney,E., Stamatoyannopoulos,J.A., Dutta,A., Guigo,R., Gingeras,T.R., Margulies,E.H., Weng,Z., Snyder,M., Dermitzakis,E.T., Thurman,R.E. *et al.* (2007) Identification and analysis of functional elements in 1% of the human genome by the ENCODE pilot project. *Nature*, **447**, 799–816.

25. Washietl,S., Pedersen,J.S., Korbel,J.O., Stocsits,C., Gruber,A.R., Hackermuller,J., Hertel,J., Lindemeyer,M., Reiche,K., Tanzer,A. *et al.* (2007) Structured RNAs in the ENCODE selected regions of the human genome. *Genome Res*, **17**, 852–864.

26. Blow,M.J., Grocock,R.J., van Dongen,S., Enright,A.J., Dicks,E., Futreal,P.A., Wooster,R. and Stratton,M.R. (2006) RNA editing of human microRNAs. *Genome Biol.*, **7**, R27.

27. Kawahara,Y., Zinshteyn,B., Chendrimada,T.P., Shiekhattar,R. and Nishikura,K. (2007) RNA editing of the microRNA-151 precursor blocks cleavage by the Dicer-TRBP complex. *EMBO Rep.*, **8**, 763–769.

28. Kawahara,Y., Zinshteyn,B., Sethupathy,P., Iizasa,H., Hatzigeorgiou,A.G. and Nishikura,K. (2007) Redirection of silencing targets by adenosine-to-inosine editing of miRNAs. *Science*, **315**, 1137–1140.

29. Knight,S.W. and Bass,B.L. (2002) The role of RNA editing by ADARs in RNAi. *Mol. Cell*, **10**, 809–817.

30. Luciano,D.J., Mirsky,H., Vendetti,N.J. and Maas,S. (2004) RNA editing of a miRNA precursor. *RNA*, **10**, 1174–1177.

31. Scadden,A.D. and Smith,C.W. (2001) RNAi is antagonized by A→I hyper-editing. *EMBO Rep.*, **2**, 1107–1111.

32. Yang,W., Chendrimada,T.P., Wang,Q., Higuchi,M., Seeburg,P.H., Shiekhattar,R. and Nishikura,K. (2006) Modulation of microRNA processing and expression through RNA editing by ADAR deaminases. *Nat. Struct. Mol. Biol.*, **13**, 13–21.

33. Pace,J.K. II and Feschotte,C. (2007) The evolutionary history of human DNA transposons: evidence for intense activity in the primate lineage. *Genome Res.*, **17**, 422–432.

34. Shen,M.R., Batzer,M.A. and Deininger,P.L. (1991) Evolution of the master Alu gene(s). *J. Mol. Evol.*, **33**, 311–320.

35. Athanasiadis,A., Rich,A. and Maas,S. (2004) Widespread A-to-I RNA editing of Alu-containing mRNAs in the human transcriptome. *PLoS Biol.*, **2**, e391.

36. Blow,M., Futreal,P.A., Wooster,R. and Stratton,M.R. (2004) A survey of RNA editing in human brain. *Genome Res.*, **14**, 2379–2387.

37. Eisenberg,E., Nemzer,S., Kinar,Y., Sorek,R., Rechavi,G. and Levanon,E.Y. (2005) Is abundant A-to-I RNA editing primate-specific? *Trends Genet.*, **21**, 77–81.

38. Kim,D.D., Kim,T.T., Walsh,T., Kobayashi,Y., Matise,T.C., Buyske,S. and Gabriel,A. (2004) Widespread RNA editing of embedded alu elements in the human transcriptome. *Genome Res.*, **14**, 1719–1725.

39. Levanon,E.Y., Eisenberg,E., Yelin,R., Nemzer,S., Hallegger,M., Shemesh,R., Fligelman,Z.Y., Shoshan,A., Pollock,S.R., Sztybel,D. *et al.* (2004) Systematic identification of abundant A-to-I editing sites in the human transcriptome. *Nat. Biotechnol.*, **22**, 1001–1005.

40. DeCerbo,J. and Carmichael,G.G. (2005) Retention and repression: fates of hyperedited RNAs in the nucleus. *Curr. Opin. Cell. Biol.*, **17**, 302–308.

41. Jepson,J.E. and Reenan,R.A. (2007) RNA editing in regulating gene expression in the brain. *Biochim. Biophys. Acta*. On line 3 Dec 2007.

42. Wang,Q., Zhang,Z., Blackwell,K. and Carmichael,G.G. (2005) Vigilins bind to promiscuously A-to-I-edited RNAs and are involved in the formation of heterochromatin. *Curr. Biol.*, **15**, 384–391.

43. Gommers-Ampt,J.H. and Borst,P. (1995) Hypermodified bases in DNA. *FASEB J.*, **9**, 1034–1042.

44. Kirnos,M.D., Khudyakov,I.Y., Alexandrushkina,N.I. and Vanyushin,B.F. (1977) 2-aminoadenine is an adenine substituting for a base in S-2L cyanophage DNA. *Nature*, **270**, 369–370.

45. Emeny,J.M. and Morgan,M.J. (1979) Regulation of the interferon system: evidence that Vero cells have a genetic defect in interferon production. *J. Gen. Virol.*, **43**, 247–252.

46. Combredet,C., Labrousse,V., Mollet,L., Lorin,C., Delebecque,F., Hurtrel,B., McClure,H., Feinberg,M.B., Brahic,M. and Tangy,F. (2003) A molecularly cloned Schwarz strain of measles virus vaccine induces strong immune responses in macaques and transgenic mice. *J. Virol.*, **77**, 11546–11554.

47. Billecocq,A., Spiegel,M., Vialat,P., Kohl,A., Weber,F., Bouloy,M. and Haller,O. (2004) NSs protein of Rift Valley fever virus blocks interferon production by inhibiting host gene transcription. *J. Virol.*, **78**, 9798–9806.

48. Levanon,E.Y., Hallegger,M., Kinar,Y., Shemesh,R., Djinovic-Carugo,K., Rechavi,G., Jantsch,M.F. and Eisenberg,E. (2005) Evolutionarily conserved human targets of adenosine to inosine RNA editing. *Nucleic Acids Res.*, **33**, 1162–1168.

49. Nishikura,K. (2006) Editor meets silencer: crosstalk between RNA editing and RNA interference. *Nat. Rev. Mol. Cell. Biol.*, **7**, 919–931.

50. Di Noia,J.M. and Neuberger,M.S. (2007) Molecular mechanisms of antibody somatic hypermutation. *Annu. Rev. Biochem.*, **76**, 1–22.

51. Cheynier,R., Henrichwark,S., Hadida,F., Pelletier,E., Oksenhendler,E., Autran,B. and Wain-Hobson,S. (1994) HIV and T cell expansion in splenic white pulps is accompanied by infiltration of HIV-specific cytotoxic T lymphocytes. *Cell*, **78**, 373–387.

52. Pham,P., Bransteitter,R., Petruska,J. and Goodman,M.F. (2003) Processive AID-catalysed cytosine deamination on single-stranded DNA simulates somatic hypermutation. *Nature*, **424**, 103–107.

53. Scadden,A.D. (2005) The RISC subunit Tudor-SN binds to hyper-edited double-stranded RNA and promotes its cleavage. *Nat. Struct. Mol. Biol.*, **12**, 489–496.

54. Schrag,S.J., Rota,P.A. and Bellini,W.J. (1999) Spontaneous mutation rate of measles virus: direct estimation based on mutations conferring monoclonal antibody resistance. *J. Virol.*, **73**, 51–54.

55. Biebricher,C.K. and Eigen,M. (2005) The error threshold. *Virus Res.*, **107**, 117–127.